Particle-induced oxidative damage by indoor size-segregated particulate matter from coal-burning homes in the Xuanwei lung cancer epidemic area, Yunnan Province, China.

Xiaolei Feng [1], Longyi Shao [1, *], Chunxiu Xi [1], Tim Jones [2], Daizhou Zhang [3], Kelly BéruBé [4]

[1] State Key Laboratory of Coal Resources and Safe Mining and College of Geoscience and Surveying Engineering, China University of Mining and Technology, Beijing 100083, China

[2] School of Earth and Ocean Sciences, Cardiff University, Museum Avenue, Cardiff, CF10, 3YE, UK

[3] Faculty of Environmental and Symbiotic Sciences, Prefectural University of Kumamoto, Kumamoto 862-8502, Japan

[4] School of Biosciences, Cardiff University, Museum Avenue, Cardiff CF10, 3US, UK

* Corresponding author. State Key Laboratory of Coal Resources and Safe Mining and College of Geoscience and Surveying Engineering, China University of Mining and Technology, Beijing 100083, PR China.

E-mail addresses:506870566@qq.com (X.L. Feng), ShaoL@cumtb.edu.cn (L.Y. Shao), 2558465218@qq.com (C.X. Xi), JonesTP@cardiff.ac.uk (T. Jones), dzzhang@pu-kumamoto.ac.jp (D.Z. Zhang), Berube@cardiff.ac.uk (K. Berube)

Highlights:

1. Indoor size-segregated particles were collected at the Hutou lung cancer epidemic village.
2. DNA damage assessed by plasmid scission assay was mainly caused by smaller particles.
3. DNA damage had a positive correlation with the water-soluble Zn, Cu, Cd, Rb, Cs, and Sb.
4. Water-soluble metals Zn, Cu, Cd, Rb, Cs, and Sb were concentrated in the smaller particles.
5. Indoor particles in the small sizes were a higher health risk than those in the large sizes.

Abstract: Size-segregated samples of airborne particulate matter were collected at the coal-burning homes of the Hutou high lung cancer epidemic village and a comparison site Xize village of the Xuanwei County, Yuanan Province, by an Anderson Cascade Impact Sampler in winter and spring to study the toxicological characteristics of different-sized particles. The DNA damage caused by the water-soluble fractions of these size-segregated particles was analyzed by the Plasmid Scission Assay, and the trace element compositions were determined by Inductively Coupled Plasma Mass Spectrometry. The DNA damage rate from the airborne particles in the high lung cancer incidence area was higher than that in Xize village. The different-sized particles have highly varying DNA damage rates, with the values being greater in the small size range than in the large size range. The particle-induced DNA damage rates had a significantly positive correlation with total water-soluble trace elements. Further analysis of the individual elements indicated that the water-soluble heavy metals Zn, Cu, Cd, Rb, Cs, and Sb had a positive correlation with the particle-induced DNA damage, implying that these water-soluble heavy metals played an important role in the DNA damage. The Sr had a negative correlation with the particle-induced DNA damage, suggesting that the water-soluble Sr might counter DNA damage. The mass concentrations of the total and individual water-soluble trace elements were mostly enriched in the small particle size ranges, thus implying the indoor airborne particles in the small size ranges would have a higher health risk.

Keywords: Xuanwei lung cancer epidemic, coal-burning emissions, indoor size-segregated particulate matter, water-soluble trace elements, plasmid scission assay

1. Introduction

Xuanwei County has attracted considerable attention due to the unusually high incidence of lung cancer levels and mortality (Zhou et al., 2006, Chen et al., 2015). A number of studies showed that tobacco smoking is not sufficient to explain the high lung cancer incidence in Xuanwei, and instead, the coal burning is closely related to this lung cancer (Barone-Adesi et al., 2012; Hosgood et al., 2013;

Shao et al., 2013; Seow et al. 2014; Lui et al., 2017; Finkelman et al., 2018). The incidence of lung cancer in Xuanwei's rural areas is the highest in China at approximately five times the national average and was highly associated with the domestic coal combustion (Mumford et al., 1987; He et al., 1994). Yang et al., (2010) found that lung cancer incidence in Xuanwei females was higher than that in Xuanwei males and non-Xuanwei females, implying that lung cancer incidence might be related to the coal burning particles emitted during cooking. The main energy source for residents in Xuanwei City is the C1 coal situated stratigraphically at the end-Permian mass extinction (Large et al., 2009; Shao et al., 2015; Wang et al., 2018) which is characterized by medium to high ash yields (averaged 31.0%), low to medium volatile contents (averaged 20.0%), low sulfur contents (averaged 0.17%), and mid-rank (with the vitrinite reflectance from 1.19% to 1.37%) (Shao et al., 2015).

The study by He and Yang, (1994) revealed that the main risk factor for the high lung cancer mortality in Xuanwei was the exposure to the high levels of carcinogenic polycyclic aromatic hydrocarbons (PAHs) (e.g., BaP) from indoor coal emissions. Tian et al., (2008) reported that the exposure variable associated with the lung cancer risk in Xuanwei was the indoor air emissions of crystalline silica. A study carried by Large et al., (2009) revealed that high silica content in coal from Xuanwei may be interacting with toxic volatiles in the coal to cause unusually high rates of lung cancer. Zhang et al., (2016) studied the particles emitted from residential coal fires and found that the toxicity caused by the fine particles is higher. A study of the characteristics of individual particles emitted by experimental combustion of the Xuanwei coals demonstrated that harmful minerals like quartz and Si-rich particles comprise the main particulate matter (Wang et al., 2019).

There are extensive studies dealing with the health effects of airborne particulate matter (PM) (Rückerl et al., 2011; Brauer et al., 2012; Balakrishnan et al., 2015; Hu et al., 2016; Wang et al., 2017; Li et al., 2020; Xing et al., 2020). Long-term exposure to $PM_{2.5}$ (i.e. PM $\leq$ 2.5 microns in aerodynamic diameter) can lead to small gestational age (Hao et al., 2019), respiratory disease (Li et al., 2013a, 2013b; Conibear et al., 2018; Slama et al., 2019), ischemic heart disease (Pope et al., 2015; Thurston et al., 2016; Shah et al., 2013), and a range of lung diseases (Chow, 2006; Araujo et al., 2011), especially in residential areas that burn large amounts of fossil fuels. Even in the case of low mass concentrations of airborne particles, pollutants still can increase exposure risk (Kim et al., 2015). Numerous studies have shown that types and levels of the metal elements in airborne particulates have important effects on health, causing lung damage in humans (Zelikoff et al., 2002; Gilli et al., 2007). Costa and Dreher (1997) noticed that biologically active transition metal elements play a greater role in lung damage, and they have suggested that the soluble metal elements in the particles are even more harmful. A study by Xue et al., (2018) has shown that a positive correlation exists between lung cancer and $PM_{2.5}$. The metal elements can be abundant in aerosols, especially in the fine particles with size ranges below 2.5μm (Schneidemesser et al., 2010).

The plasmid scission assay is an *in vitro* particle toxicology method employed to study oxidative damage of supercoiled DNA by free radicals (Greenwell et al., 2002; Moreno et al., 2004; Shao et al., 2013), and has been widely used to assess the oxidative capacity of airborne PM (Chuang et al., 2015; Shao et al., 2016; Shao et al., 2017). Several studies have noted that the DNA damage caused by water-soluble components in airborne particulates is significant (Merolla et al., 2005; Shao et al., 2013; Hou et al., 2016).

Trace elements and their concentrations can differ in particles of different sizes and can thus have different impacts on human health (Cao et al., 2012; Chow et al., 2012; Duan et al., 2012; Sun et al., 2014; Rohra et al., 2018). Particles with small sizes are of more concern due to their large specific surface area and strong adsorption capacity, leading to the enrichment of heavy metals in the smaller particles (Al-Dabbous et al., 2018; Olawoyin et al., 2018). Pan et al., (2015) have found that the toxic trace element content in northern China were concentrated in the submicron (<1.1μm in aerodynamic diameter) particle size range. Although the association of the water-soluble elements with the DNA damage in the particulate matter in a Xuanwei high lung cancer incidence area has been demonstrated by Shao et al., (2013), the size-segregated particulate matter, the size distribution of the water-soluble trace elements and the particle-induced DNA damages are poorly understood.

The human respiratory system (RS) is perpetually exposed to oxidants generated either endogenously or exogenously (e.g. indoor and outdoor combustion-derived PM; CDPM). Reactive oxygen species (ROS) and oxidative stress in the RS increases the production of inflammatory mediators that promote carcinogenic mechanisms. The risk of developing lung cancer increases substantially following exposure to CDPM due to the synergistic effects in the generation of ROS and concomitant induction of oxidative stress and inflammation that culminates in an elevated DNA damage potential (IARC, 2012). PM physico-chemistry (e.g. size, shape, solubility, transition metal content, speciation, stable free radicals, etc.) plays an important role in its oxidative capacity (Hamra et al., 2014). PM-induced ROS initiates the synthesis of mediators of inflammation in lung epithelial cells and initiation of carcinogenic mechanisms (DEFRA, 2017).

In this study, we collected airborne particles of different sizes in a high lung cancer incidence village and a comparison village in Xuanwei County. The mass concentration and oxidative damage characteristics of PM in different particle size ranges were analyzed. The distribution of the water-soluble trace elements in the different particle sizes were also investigated, and their relationships with the plasmid DNA damage rates were studied in order to identify the major heavy metal elements and the major particle size ranges which are more closely associated with the DNA damage.

2. Materials and methods

2.1. Sampling

The samples were collected from Hutou village in Xuanwei, an area with high-risk lung cancer, and Xize village, a low-risk comparison site. The sampling campaign was divided into two periods. One was in December 2016 during winter when the coal is extensively used, and the other was in March 2019 during spring when the coal is used less, both of which had same sampling sites. The sampler was placed in the kitchens of two villagers' apartments in Hutou village (Hutou I, Hutou II) and one villager's apartment in Xize village. Coal was used as the fuel at all sampling sites. The selected sampling point will only burn coal for cooking during the winter and did not use coal at other times during the spring. Xize village only burns coal for cooking. The sampling equipment was an eight-stage Anderson cascade impact sampler (TE-20-800 TISCH, Germany), with a sampling height 1.5m above the ground. Quartz filters (80mm diameter, Millipore, China) were used for sampling. The sampling flow rate was 28.3L/min, and the sampler segregated particles in eight size ranges: 0.43-0.65μm, 0.65-1.1μm, 1.1-2.1μm, 2.1-3.3μm, 3.3-4.7μm, 4.7-5.8μm, 5.8-9.0μm and 9.0-10μm.

Before sampling, the quartz filters were heated at 450°C for 4 hours and placed in a constant temperature and humidity chamber (Hitachi, Japan; temperature: 20°C ± 5°C, relative humidity: 45% ± 5%). After the samples were collected, they were placed in the constant temperature and humidity chamber for 48 hours before weighing. The mass concentrations of the different size particles were obtained using the gravimetric method. The blank filters and the sample-loaded filters were weighed using an electronic balance (MS105DU, Switzerland) with an accuracy of 0.01mg. The mass concentration of the sample was calculated according to the sampling flow rate as follows:

$$C = \frac{W_2 - W_1}{Vs}$$

$$Vs = \frac{P \times V \times 273}{1013.25 \times (273 + T)}$$

Where: C-sample mass concentration (g/m^3), Vs-standard sample volume (m^3), W_1-weight of quartz membrane before sampling (g), W_2-weight of quartz membrane after sampling (g), V-actual sampling volume (m^3), P-average air pressure (hPa), T-sampling average temperature (°C).

Simultaneously, a portable meteorological instrument (Kestrel 5500 Weather LiNK, USA) was used throughout the sampling process to monitor meteorological conditions including temperature, relative humidity, and pressure. The sample information and the meteorological conditions during the sampling period are shown in Table 1.

2.2. Plasmid DNA scission assay

The plasmid DNA assay is an *in vitro* method to measure oxidative damage to plasmid DNA induced by free radicals on the particle surface. Oxidative damage initially causes the supercoiled DNA to relaxed and further damage results in linearization (Figure 1). The sum of the percentage of relaxed DNA and linearized DNA is the oxidative damage rate. Ultra-pure water (conductivity 18.2 MΩ, Millipore, China) was used as a procedure blank throughout the experiment. Ultra-pure water's effect on DNA was subtracted to calculate the particle oxidative damage rate. Four samples were used for each test to verify experiment accuracy. The methodological steps are as follows:

(1) Sample preparation process: Each filter (along with a corresponding blank filter) was cut into half, and the mass of each sample was calculated. The sample was immersed in ultra-pure water. The sample solution was gently shaken for 20 hours in a shaker (VORTEX-GENIE2, Scientific Industries, USA) and then sonicated for 2 min. This released the particulate matter from the filter substrate into the solution. After this step, the sample solution was centrifuged (D-37520 Osterode, Germany) to deposit particles at the bottom of the tube, then, the mixture supernatant was taken as water-soluble sample. The water-soluble sample was adjusted to a 250μg/mL dose level. 4μl of X174-RF DNA (Promega, USA) was added.

(2) Gel preparation: Tris/Borate/EDTA (TBE) buffer solution (Thermo Scientific, China) diluted 10 times with agarose (molecular biology grade; Sigma-Aldrich, China) was mixed, and the solution

was heated to clarity and transparency. The solidified gel was placed in an electrophoresis cell (DYCP-34C; LIUYI, China) containing ten-times diluted TBE buffer.

(3) Injection of DNA mixtures and sample into the gel: 14μL of bromophenol blue stain (Sigma-Aldrich, China) was added to the sample. After rocking horizontally for 6 hours in a rocker (HX-3000, YOUNING, China), a fixed volume pipette (Eppendorf, Germany) was used to load 20μL of the solution into each gel well. Four parallel samples were made for each sample. 20μL of ethidium bromide (EB; Sigma-Aldrich, China) was added to both sides of the electrophoresis tank. After the EB was fully dissolved in the buffer, the laboratory electrophoresis power supply (DYY-6C, LIUYI, China) was turned on and operated at 30 Volts for 16 hours.

(4) Gel imaging and quantitative analysis of oxidative DNA damage: After 16 hours, the optical densities of three different DNA morphologies (i.e. super-coiled, relaxed and linear) in the gel were captured using a gel documentation system (ChemiDoc, Bio-red, China) and the Genetools (version 4.0; Syngene, USA) image analysis software program was utilized to determine the damage rate of DNA via a linear regression analysis. In the final calculation, the DNA damage of ultra-pure water was subtracted from the DNA damage caused by particles.

2.3. Inductively coupled plasma mass spectrometer (ICP-MS)

The water-soluble samples obtained by the first step of Plasmid DNA scission assay were also chemically analyzed by inductively coupled plasma mass spectrometry (ICP-MS, 7700x, Agilent Ltd.). Chemical analysis of the water-soluble sample using ICP-MS identified 26 elements with values above the detection limit. The trace element content (ng/mL), the solution volume (mL), and the actual sample volume in the water-soluble sample were calculated according to the following formula to obtain the mass concentration (ng/m^3) of the water-soluble element.

$$C = \frac{c \times Vt}{V}$$

Where: *C* represents the mass concentration of water-soluble trace elements (ng/m^3), *c* represents the trace element content in the water-soluble sample (ng/mL), *Vt* represents the volume of the ~~measured~~ total solution (mL), *V* represents the actual volume at the time of sampling (m^3).

3. Results and Discussion

3.1 Mass concentrations of size-segregated particles

The mass concentrations of size-segregated particles are presented in Table 2. The PM mass concentration in winter was greater than that in spring in the Hutou village, and the total PM mass concentrations at Hutou in both winter and summer were all significantly higher than that in the Xize village.

The mass concentrations of PM had a clear size distribution (Table 2) with the PM mass concentration decreasing first and then increasing with increased particle size. Due to sampler effects, particles in the large size range may fall into the small size collections, resulting in abnormally high values of the particle mass concentration in the 0.65-1.1μm range.

For Hutou I, the winter sample showed that the PM mass concentration decreased first and then increased with increased particle size, while the spring sample showed that the PM mass concentration continuously increased with the increase of particle size. The winter sample had the lowest mass concentration value (27.10μg/m^3) in the 2.1-3.3μm range and the maximum value (67.17μg/m^3) in the 9.0-10μm range. The spring sample had the lowest mass value (24.17μg/m^3) in the 0.43-0.65μm and maximum values (62.78μg/m^3) in the 9.0-10μm ranges, with the maximum value being in the same size range as the winter sample (Figure 2).

For Hutou II, both winter and spring samples showed that the PM mass concentration decreased first and then increased with increased particle size. The winter sample had the lowest value (24.86μg/m^3) in the 2.1-3.3μm range and the maximum value (44.56μg/m^3) in the 0.43-0.65μm range. The spring sample had the lowest value (21.29μg/m^3) in the 2.1-3.3μm range and the highest value (42.11μg/m^3) in the 9.0-10μm range (Figure 2).

In Xize village, the PM mass concentration also decreased first and then increased with increased particle size, the same as the Hutou II and the winter sample of Hutou I. It had the lowest value (3.51μg/m^3) in the 2.1-3.3μm range and the highest value (32.93μg/m^3) in the 0.43-0.65μm range (Figure 2).

A comparison of the PM mass-size distribution at the sampling sites in Hutou and Xize villages revealed that the Hutou samples had a higher value in the 0.65-10μm range and a lower value in the 0.43-0.65μm range than the Xize sample (Figure 2).

The large particles in the 5.8-10μm size range are deposited in the nasal cavity, and the small particles in the 0.43-2.1μm size range enter the bronchi (Sridevi et al., 2017) and the particles in the 2.5-5μm have a larger residence time than the particles in the 5-10μm (Schleicher et al., 2011). Comparing the winter and spring samples of Hutou village, the winter sample mass concentration contains significant smaller particles, indicating that coal combustion has a significant impact on indoor air quality. One possible explanation could be that there is more ambient airborne during the spring. For both the small and large particle in the winter sample at the three sampling sites, the PM mass concentration in Hutou is higher than that in Xize (in Figure 3).

3.2 Oxidative capacity of the size-segregated airborne particles

Numerous studies have demonstrated that the oxidative capacity of the whole particle suspensions were similar to those of the water-soluble fractions, indicating that the DNA damage induced by particulate matter was mainly a result of the water-soluble fraction (Shao et al., 2013, 2016). Therefore, we analyzed the oxidative capacity of the water-soluble components of size-segregated particles of the collected samples.

For the comparison study, the DNA damage rate at the particle dosage of 250μg/mL was taken for the size-segregated particles (Table 3). It can be seen that the damage rates of the Hutou samples at this dosage were generally higher than those of the Xize samples, and the damage rates of all the winter samples were generally higher than those of the all spring samples in the Hutou village. It is also clear that the damage rates of the samples in the small size ranges, mostly 0.43-1.1μm, were higher than those in the 9-10μm size ranges. Although the damage rates increased slightly in the 5.8-10μm size range, they were still lower than the damage rates caused by the small size ranges. Sun et al., (2014) studied the haze and clear weather PM in Beijing, they found that the average damage rate in the 0.32-1.8μm size ranges was higher than that in the 5.6-10μm size ranges. This is similar to the case in Xuanwei where the DNA damage rate caused by small particles is also greater than that caused by large particles.

It can also be seen in Table 3 that the DNA damage rates of the winter samples of Hutou village were higher than those of Xize village, but those of the spring samples of Hutou I particles in the 4.7-5.8μm size range and Hutou II in the 0.65-3.3μm size range were lower than the those of Xize particles in the corresponding size ranges.

3.3 Relationship between water-soluble trace element content and the particle-induced DNA damage of the size-segregated particles

To examine the most probable source of the particle-induced oxidative capacities of the PM samples, the DNA damage rates from particle doses of 250μg/ml were correlated against the corresponding contents of the total and individual water-soluble elements in the PM (Table 4). According to the correlation analysis, the coefficient is higher than 0.393 at the 0.01 significance level with a sample number N = 40, which indicates that these two factors are related.

It can be seen in Table 4 that there is a significant positive correlation between the DNA damage rates and the contents of total water-soluble trace elements, with the correlation coefficient of 0.649, being higher than the critical value of 0.393. This demonstrated that the particle-induced DNA damage was mainly caused by the water-soluble elements.

The individual elements Zn, Cu, Cd, Rb, Tl, Cs, and Sb showed a significant correlation with DNA damage rates, all of which had correlation coefficients higher than the critical value. Among these elements, the correlation coefficients of Cu (0.639), Zn (0.679), Tl (0.681), and Rb (0.690) were particularly high. Opposite to these elements, the Sr had a negative correlation with the particle-induced DNA damage, being -0.428, implying that the water-soluble Sr might mediate DNA damage.

3.4 Mass concentrations and health risk of total water-soluble elements for the size-segregated particles

The correlation between the water-soluble elements and the oxidative DNA damage (Table 4) revealed that the total water-soluble elements, together with the individual elements Zn, Cu, Cd, Rb, Tl, Cs, and Sb, were positively associated with the oxidative potential. Therefore, the mass concentrations of the total water-soluble elements and these individual Positively Correlated Water-Soluble Elements (PCWSE) could represent the health risk levels of PM exposure.

Table 5 presents the total water-soluble element mass concentration (ng/m^3) of size-segregated particles. It can be seen that the total water-soluble elements mass concentration in winter was greater than that in spring for the two sampling sites in the Hutou village. The value for the winter in the Xize village was very low compared to that for the winter in Hutou village, and this is mainly due to less coal being burnt during winter.

The mass concentrations of the total water-soluble elements had a clear size distribution (Table 5). For Hutou I, the mass-size distribution of the total water-soluble elements of the winter samples had the highest mass value (333.83ng/m^3) in the 0.43-0.65μm range and the lowest mass value (9.02ng/m^3) in the 4.7-5.8μm range. The spring samples showed the highest mass value of the total water-soluble elements (15.44ng/m^3) in the 0.65-1.1μm range and the lowest value (0.53ng/m^3) in the 9.0-10μm range. Both the winter and spring samples demonstrated that the water-soluble elements were enriched in the fine particle size range (Table 5). This is an agreement with the mass-size distribution of trace elements in Xuanwei (Lv et al., 2017).

For Hutou II, the mass-size distribution of the total water-soluble elements of the winter sample showed the highest value (21.47ng/m^3) in the 1.1-2.1μm range and the lowest value (6.26ng/m^3) in the 4.7-5.8μm range. The spring sample had the highest value (10.56ng/m^3) in the 1.1-2.1μm range and the lowest value (0.45ng/m^3) in the 0.43-0.65μm range.

In Xize village, the mass-size distribution of the total water-soluble elements showed the highest value (21.69ng/m^3) and the minimum value (2.93ng/m^3) were in the 0.65-1.1μm range and 2.1-3.3μm range, respectively.

In general, the mass-size distribution of the total water-soluble elements in Xuanwei area showed a higher value in the smaller than 2.1μm size range, and a lower value in the larger than 4.7μm size range, indicating that the water-soluble elements tended to be enriched in the smaller particles. This indicates that the indoor airborne particles in the small size ranges would have a higher health risk than those in the large size ranges.

3.5 Mass concentrations and health risk of individual water-soluble elements for the size-segregated particles

Among the analyzed elements, Zn, Cu, Cd, Rb, Tl, Cs, and Sb showed a positive correlation, and Sr showed a negative correlation with the particle-induced DNA damage. The mass-size distribution of these individual water-soluble trace elements in particles for the five sets of samples at three sampling sites were further analyzed.

Figure 4a and 4b showed the mass concentrations of Zn generally decreased with the increase of the particle sizes. It can be seen that Zn was mostly concentrated in the particle size range less than 2.1μm, although some variation existed in the Hutou I spring sample. Zn is a major trace element contributing to DNA damage rate in Beijing's atmosphere (Shao et al., 2013, 2017). Rönkkö et al., (2018) found that the mass concentration of Zn in $PM_{2.5\text{-}1.0}$ is high in Nanjing's atmosphere. In the United States of America, Zn was also found to have the highest concentration in the fine particle size range (PM≤2.5μm) (Olawoyin et al., 2018). In a study on the mass-size distribution of the individual water-soluble trace elements in size-segregated airborne particles, Zn was found to be concentrated in the range of 0.56–1.0μm (Sun et al., 2014). These results were also in good agreement with previous studies in Beijing by Xu et al., (2007) and Duan et al., (2012) and in Shenyang by Hong et al., (2011).

Figure 5a and 5b showed the mass concentrations of Cu. In the Hutou I winter sample, Cu was mostly concentrated in the smaller than 2.1μm particle size range, and in all other samples, a general decrease in mass concentration with the increase of the sizes, although some variation existed. The Hutou II winter sample had an increase in the concentration in the larger than 5.8μm particles. The study on the mass-size distribution of the individual water-soluble trace elements in size-segregated airborne particles has demonstrated that Cu was concentrated in the range of 0.56–1.0μm (Sun et al., 2014), which is in a good agreement with this study. Wang et al., (2016) studied the enrich of the heavy elements in Jincheng dust, indicating that they were affected by human activities.

Figure 6a and 6b showed that concentrations of Cd generally decreased with the increase of the particle sizes. In the Hutou I and Hutou II winter samples Cd was mostly concentrated in the particles smaller than 4.7μm, and in all other samples, Cd was concentrated in the particles smaller than 2.1μm. The mass-size distribution of Cd is similar to the distribution of trace metals in the British atmosphere (Allen et al., 2001). The International Agency for Research on Cancer identified that Cd is in a class of substances that are carcinogenic to humans (IARC, 2017). Rönkkö et al., (2018) also found the mass concentration of Cd in $PM_{2.5}$ is high in Nanjing's atmosphere.

Figure 7 and Figure 8 showed variation in concentrations of Rb, Tl, Cs and Sb. It can be seen in the five samples that the mass-size distributions of Rb, Tl and Cs generally decreased with the increase of the particle sizes, and all samples showed that Rb and Tl were both enriched in the particles smaller than 2.1μm and Cs was enriched in the particles smaller than 1.1μm (Figure 7a and 7b and Figure 8a). Figure 8b showed that the mass concentration of Sb had an overall decrease with the increase of the particle sizes, except the Hutou II spring sample, which showed some variation, and the Xize sample, which had a small increase in the particle size range of 9-10μm. Ma et al., (2019) studied the water-soluble particulate elements in the coastal city of Marina, California, and found that Rb exhibited concentration peaks in the 0.32-0.56μm size range. Lv et al., (2017) found that Tl concentrates in PM2.1 and Sb has a dominant peak in the particles smaller then 2.1μm in the nonferrous metal smelting industry of Zhuzhou, Hunan province. Tan et al., (2016) found the mass concentrations of Cs and Sb were enriched in the particles smaller than 1μm in a high polluted episode during winter in Beijing.

Figure 9a and 9b showed the mass-size distribution of Sr. Opposite to all the other elements, Sr showed an obvious increasing trend with the particle sizes and higher values were concentrated in the large particle sizes. Tang et al., (2018) studied the office indoor air in Nanjing and found that Sr was concentrated in the particles larger than 5.8μm. Tan et al., (2016) also found the mass concentration of Sr was enriched in the particles larger than 2.7μm in a high pollution episode during winter in Beijing.

3.6 The comparison of the water-soluble trace elements in the airborne particles with other regions

The mass concentrations of the water-soluble trace elements in the airborne particles in the Hutou lung cancer epidemic village were very high, especially those having positive correlations with the DNA damage. We have compared the Xuanwei data with those of the megacities of Beijing, Guangzhou and Harbin in Table 6. It can be seen that the mass concentrations of both total and most individual water-soluble trace elements in the PM collected in Xuanwei were much higher than those in other cities. In particular, the mass concentrations of the water-soluble heavy metals Zn, Cu, Cd which potentially caused the particle-induced DNA damage were significantly higher than those in Beijing, Guangzhou, and Harbin.

4. Conclusions

1) The PM mass concentration in winter was greater than that in spring in the Hutou lung cancer village, and PM mass first and then increases with increased particle size.

2) The DNA damage rate of Hutou samples was higher than that of Xize samples. The damage rate of the winter sample is higher than that of the less coal-burning spring sample in Hutou village. The damage rate in the smaller than 2.1μm size range was greater than the damage rate in the large

size range.

3) The total water-soluble elements, together with the individual elements Zn, Cu, Cd, Rb, Tl, Cs, and Sb, were positively associated with the oxidative potential, suggesting that these elements could be a main cause for the particle-induced DNA damage. Sr had a negative correlation with the DNA damage rate, implying this element might inhibit the DNA damage.

4) The mass concentrations of the total and individual water-soluble trace elements were mostly enriched in the small particle size ranges, thus implying the indoor CDPM in the small size ranges would have a higher health risk.

5) A comparison analysis indicates that the mass concentrations of the water-soluble heavy metals Zn, Cu, Cd which potentially caused the particle-induced DNA damage were significantly higher in Xuanwei area than those in Beijing, Guangzhou, and Harbin.

6) Pulmonary cancer initiation and promotion has been directly linked to biochemical pathways of oxidative stress and DNA oxidative damage that modulates gene expression and activation of transcription factors with important roles in carcinogenesis.

Author contribution statement

Xiaolei Feng: Sample, Conceptualization, Methodology, Formal analysis, Writing - Original Draft. Longyi Shao: Conceptualization, Supervision, Resources, Writing - Review & Editing, Project administration, Resources, Funding acquisition. Chunxiu Xi: Project administration, Sample. Tim Jones: Date Analysis, Geochemistry, Editing. Daizhou Zhang: Editing. Kelly BéruBé: Date Analysis, Toxicology, Editing.

Acknowledgments

This study is supported by the National Natural Science Foundation of China (Grant No. 41572090), the Projects of International Cooperation and Exchanges NSFC (Grant No. 41571130031) and the Yueqi Scholar fund of China University of Mining and Technology (Beijing).

References

Al-Dabbous, A.N., Kumar, P., 2014, Number size distribution of airborne nanoparticles during summertime in Kuwait: First observations from the Middle East. *Environmental Science & Technology 48*, 13634-43.

Allen, A.G., Nemitz, E., Shi, J.P., Harrison, R.M., Greenwood, J.C., 2001, Size distributions of trace metals in atmospheric aerosols in the United Kingdom. *Atmospheric Environment 35*, 4581-4591.

Ambient air quality standards, 2012.

Araujo, J.A., 2011, Particulate air pollution, systemic oxidative stress, inflammation, and atherosclerosis. *Air Quality Atmosphere Health 4*:79–93.

Balakrishnan, K., Sambandam, S., Ramaswamy, P., Ghosh, S., Venkatesan, V., Thangavel, G., Mukhopadhyay, K., Johnson, P., Paul, S., Puttaswamy, N., Dhaliwal, R.S., SRU-CAR Team, 2015, Establishing integrated rural-urban cohorts to assess air pollution–related health effects in pregnant women, children and adults in Southern India: An overview of objectives, design and methods in the Tamil Nadu Air Pollution and Health Effects (TAPHE) study. BMJ Open.

Barone-adesi, F., Chapman, R.S., Silverman, D.T., He, X., Hu, W., Vermeulen, R., Ning, B.F., Joseph, F.F., Nathaniel, R., Lan, Q., 2012, Risk of lung cancer associated with domestic use of coal in Xuanwei, China: retrospective cohort study. *Bmj British Medical Journal, 345(aug29 2)*, e5414.

Brauer, M., Amann, M., Burnett, R.T., Cohen, A., Dentener, F., Ezzati, M., Henderson, S.B., Krzyzanowski, M., Martin R.V., Dingenen, R.V., Donkelaar, A.V., Thurston, G.D., 2012, Exposure assessment for estimation of the global burden of disease attributable to outdoor air pollution. *Environmental Science & Technology 46,* 652-660.

Cao, J.J., Xu, H., Xu, Q., Chen, B., Kan, H., 2012, Fine particulate matter constituents and cardiopulmonary mortality in a heavily polluted Chinese city. *Environmental Health Perspectives 120*, 373-378.

Chang, L.L., 2019, Study on the trace elements and toxicology of $PM_{2.5}$ after the action for comprehensive control of air pollution. China University of Mining and Technology, Beijing. (in Chinese with English Abstract)

Chen, G., Sun, X., Ren, H., Wan, X., Huang, H., Ma, X., Ning, B.F., Zou, X.N., Hu, W.J., Yang, G.H., 2015, The mortality patterns of lung cancer between 1990–2013 in Xuanwei, China. *Lung Cancer 90*, 155-160.

Chow, Judith C., 2006, Health effects of fine particulate air pollution: Lines that connect. *Journal of the Air & Waste Management Association 56(6)*:707–708.

Chow, Judith C., Cao, J.J, Li, S.C., Wang, X.L., Watson, J.G., 2012, A brief history of $PM_{2.5}$, its measurement and adverse effects. *Journal of Earth Environment 5*, 1019-1029. (in Chinese with English abstract)

Chuang, H.C., Jones, T.P., Lung, S.C., BéruBé K.A., 2015, Soot-driven reactive oxygen species formation from incense burning. *Science of the Total Environment 409*, 4781-4787.

Conibear, L., Butt, E.W., Knote C.J., Arnold, S., Spracklen, D.V., 2018, Residential energy use emissions dominate health impacts from exposure to ambient particulate matter in India. *Nature Communications, 9*.

Costa, D.L., Dreher, K.L., 1997, Bioavailable transition metals in particulate matter mediate cardiopulmonary injury in healthy and compromised animal models. *Environmental Health Perspectives 105*: 1053–1060.

Department for Environment, Food and Rural Affairs (DEFRA). Air Pollution in the UK (2017)

Duan, J., Tan, J., Wang, S., Hao, J., Chai, F.H., 2012, Size distributions and sources of elements in particulate matter at curbside, urban and rural sites in Beijing. *Journal of Environmental Sciences, 24*, 87–94.

Fan, J.S., Shao, L.Y., Li, Z.X., Hu, Y., Hou, C., 2013, Mass concentration distribution of inhalable particulates in different villages Xuanwei county, China. *Applied Mechanics and Materials 295-298*, 539-542.

Finkelman R.B., Tian, L.W., 2018, The health impacts of coal use in China. *International Geology*

Review, 60, 579-589.

Gilli, G., Traversi, D., Rovere, R., Pignata, C., Schilirò T., 2007, Chemical characteristics and mutagenic activity of PM_{10} in Torino, a Northern Italian City. *Science of the Total Environment 385*, 97-107.

Greenwell, L. L., Moreno, T., Jones, T. P., Richards, R. J., 2002, Particle-induced oxidative damage is ameliorated by pulmonary antioxidants. *Free Radical Biology and Medicine 32*, 898-905.

Hamra, G.B., Guha, N., Cohen, A., Laden, F., Raaschou-Nielsen, O., Samet, J.M., Vineis, P., Forastiere, F., Saldiva, P., Yorifuji, T., Loomis, D., 2014, Outdoor particulate matter exposure and lung cancer: a systematic review and meta-analysis. *Environmental health perspectives 122*, 906-911

Hao, J., Zhang, F., Chen, D., Liu, Y., Liao, L., Shen, C., Liu, T.Y., Liao, J.L., Ma, L., 2019, Association between ambient air pollution exposure and infants small for gestational age in Huangshi, China: a cross-sectional study. *Environmental Science and Pollution Research 26*, 32029-32039

He X.Z., Yang R.D., 1994, Yunnan Science and Technology Press.

He, X., Chapman, R.S., Yang, R., Cao, S., Mumford, J.L., Liang, C., 1987, Lung cancer and indoor air pollution in Xuanwei, China: current progress. *Science 235*, 217-220.

He, X.Z., Yang, R.D., 1994, Lung Cancer and Indoor Air Pollution from Coal Burning. Yunnan Science and Technology Publishing House, Kunming (in Chinese).

Hong Y, Ma Y J, Li C L, Liu N W, Gao S P, Zhang Y H, 2011. Elemental size distribution characteristics of atmospheric particles on hazy days during winter in Shenyang. *Research of Environmental Sciences, 24(6)*, 637–643. (in Chinese with English abstract)

Hosgood, H.D., Chapman, R.S., He, X.Z., Hu, W., Tian, L.W., Liu, L.Z., 2013, History of lung disease and risk of lung cancer in a population with high household fuel combustion exposures in rural China. *Lung Cancer 81*: 343–346.

Hou, C., Shao, L.Y., Wang, J., Liu, J.X., Zhao, C.M., Geng, C.M., 2016, Distribution of trace elements in inhalable particulate matter emitted from coal burning. *Journal of China Coal Society 41*:760 −

768. (in Chinese with English abstract)

Hu Y., 2016, Domestic Coal Combustion Emissions and the Lung Cancer Epidemic in Xuanwei, China. China University of Mining and Technology, Beijing. (in Chinese with English Abstract)

International Agency for Research on Cancer (IARC). Air pollution and Cancer. Vol 161, 2012.

International Agency for Research on Cancer (IARC). World Health Organization, 2017.

Kim, K. H., Kabir, E., Kabir, S., 2015, A review on the human health impact of airborne particulate matter. *Environment International 74,* 136-143.

Large, D.J., Kelly, S., Spiro, B., Tian, L.W., Shao, L.Y., Finkelman, R., Zhang, M.Q., Somerfield, C., Plint, S., Ali, Y., Zhou, Y.P., 2009, Silica-volatile interaction and the geological cause of the Xuanwei lung cancer epidemic. *Environmental Science and Technology 43*, 9016-9021.

Li, P., Xin, J.Y., Wang, Y.S., Wang, S.G., Shang, K.Z., Liu, Z.R., Li, G.X., Pan, X.C., Wei, L.B., Wang, M.Z., 2013, Time-series analysis of mortality effects from airborne particulate matter size fractions in Beijing. *Atmospheric Environment 81*, 253-262.

Li, P., Xin, J.Y., Wang, Y.S., Wang, S.G., Li, G.X., Pan, X.C., Liu, Z.R., Wang, L.L., 2013, The acute effects of fine particles on respiratory mortality and morbidity in Beijing, 2004-2009. *Environmental Science and Pollution Research 20,* 6433-6444.

Li, Y.W., Shao, L.Y., Wang, W.H., Zhang, M.Y., Feng, X.L., Li, W.J., Zhang, D.Z., 2020. Airborne fiber particles: Types, size and concentration observed in Beijing, *Science of The Total Environment 705*, 135967.

Liu, Y.F., 2010, PM_{10} and $PM_{2.5}$ in Harbin Air: Physicochemistry and Bioreactivity. China University of Mining and Technology, Beijing. (in Chinese with English Abstract)

Lui, K.H., Bandowe, B.A.M., Tian, L.W., Chan, C.S., Cao, J.J., Ning, Z., Lee, S.C., Ho, K.F., 2017, Cancer risk from polycyclic aromatic compounds in fine particulate matter generated from household coal combustion in Xuanwei, China. *Chemosphere 169*, 660–668.

Lv, Y., Zhang, K., Chai, F.H., Cheng, T.T., Yang, Q., Zheng, Z.L., Li, X., 2017, Atmospheric size-resolved trace elements in a city affected by nonferrous metal smelting: Indications of respiratory deposition and health risk. *Environmental Pollution 224*, 559-571.

Ma, L., Dadashazar, H., Braun, R.A., MacDonald, A.B. Aghdam, M.A., Maudlin, L.C., Sorooshian, A., 2019, Size-resolved characteristics of water-soluble particulate elements in a coastal area: Source identification, influence of wildfires, and diurnal variability. *Atmospheric Environment 206*, 72-84.

Merolla, L., Richards, R. J., 2005, In vitro effects of water-soluble metals present in UK particulate matter. *Experimental Lung Research 31,* 671-683

Moreno, T., Merolla, L., Gibbons, W., Greenwell, L., Jones, T., Richards, R., 2004, Variations in the source, metal content and bioreactivity of technogenic aerosols: a case study from Port Talbot, Wales, UK. *Science of the Total Environment 333*, 59-73.

Olawoyin, R., Schweitzer, L., Zhang, K., Okareh, O., Slates, K., 2018, Index analysis and human health risk model application for evaluating ambient air–heavy metal contamination in Chemical Valley Sarnia. *Ecotoxicology and Environmental Safety 148*, 72-81.

Pan, Y.P., Tian, S.L., Li, X.R., Sun, Y., Li, Y., Wentworth, G.R., Wang, Y.S, 2015, Trace elements in particulate matter from metropolitan regions of northern China: Sources, concentrations and size distributions. *Science of The Total Environment 537*, 9-22.

Pope, C.A., Turner, M.C., Burnett, R.T., Jerrett, M., Gapstur, S.M., Diver, W.R., Krewski, D., Brook, R. D., 2015, Relationships between fine particulate air pollution, cardiometabolic disorders, and cardiovascular mortality novelty and significance. *Circulation Research 116,* 108.

Qiao, Y.S., 2011, Study on the physicochemistry and toxocity of inhalable parriculates in the Central China City Group. China University of Mining and Technology, Beijing. (in Chinese with English Abstract)

Rohra, H., Tiwari, R., Khare, P., Taneja, A., 2018, Indoor-outdoor association of particulate matter and bounded elemental composition within coarse, quasi-accumulation and quasi-ultrafine ranges in residential areas of northern India. *Science of the Total Environment 631-632*, 1383-1397.

Rönkkö T. J., Jalava, P. I., Happo, M. S., Stefanie, K., Olli, S., Ari, L., et al., 2018, Emissions and atmospheric processes influence the chemical composition and toxicological properties of urban air particulate matter in Nanjing, China. *Science of The Total Environment 639*, 1290-1310.

Rückerl, Regina, Schneider, A., Breitner, S., Cyrys, J., Peters, A., 2011, Health effects of particulate air pollution: A review of epidemiological evidence. *Inhalation Toxicology 23*, 555-592.

Schneidemesser, E.V., Stone, E.A., Quraishi, T.A., Shafer, M. M., Schauer, J.J., 2010, Toxic metals in the atmosphere in Lahore, Pakistan. *Science of the Total Environment 408*, 1640-1648.

Schleicher, N., Norra, S., Dietze, V., Yu, Y., Fricker, M., Kaminski, U., Chen, Y., Cen, K., 2011, The effect of mitigation measures on size distributed mass concentrations of atmospheric particles and black carbon concentrations during the Olympic Summer Games 2008 in Beijing. *Science of the Total Environment 412-413*, 185-193.

Seow, W.J., Hu, W., Vermeulen, R., Iii, H. H., Sdownward, G., Schapman, R., He, X.Z., ABassig, B., Kim, C., Wen, C.J., Rothman, N., Lan, Q., 2014, Household air pollution and lung cancer in China: a review of studies in Xuanwei. *Chinese Journal of Cancer 33*, 471-475.

Shah ASV, Langrish J.P., Nair H., McAllister D.A., Hunter A.L., Donaldson K., Newby, D.E., Mills, N.M., 2013, Global association of air pollution and heart failure: a systematic review and meta–analysis. *The Lancet 382*, 1039–48.

Shao, L.Y., Hu, Y., Wang, J., Hou, C., Yang, Y., Wu, M., 2013, Particle-induced oxidative damage of indoor PM_{10} from coal burning homes in the lung cancer area of Xuanwei, China. *Atmospheric Environment 77*, 959-967.

Shao, L.Y., Wang, J., Hou, H.H., Zhang, M.Q., Wang, H., Spiro, B., Large, D., Zhou, Y.P., 2015, Geochemistry of the C_1 coal of the latest Permian during mass extinction in Xuanwei, Yunnan. *Acta Geological sinica 89*, 163-179. (in Chinese with English abstract)

Shao, L.Y., Hou, C., Geng, C.M., Liu, J.X., Hu, Y., Wang, J., Jones, Tim, Zhao, C.M., BéruBé, K., 2016, The oxidative potential of PM_{10} from coal, briquettes and wood charcoal burnt in an experimental domestic stove. *Atmospheric Environment 127*, 372-381.

Shao, L.Y., Hu, Y., Shen, R.R., Schäfer, K., Wang, J., Wang, J.Y., Schnelle-Kreis, J., Zimmermann, R., BéruBé, K., Suppan, P., 2017, Seasonal variation of particle-induced oxidative potential of airborne particulate matter in Beijing. *Science of The Total Environment 579*, 1152-1160.

Slama, A., Sliwczynski, A., Woznica, J., Zdrolik, M., Wisnicki, B., Kubajek, J., Thurźańska-Wieczorek, O., Gozdowski, D., Wierzba, W., Franek, E., 2019, Impact of air pollution on hospital admissions with a focus on respiratory diseases: a time-series multi-city analysis. *Environmental Science and Pollution Research 26*, 16998-17009

Sridevi, J., Gurdeep, S., 2017, Human health risk assessment of airborne trace elements in Dhanbad, India. *Atmospheric Pollution Research 8*, 490-502.

Sun, Z.Q., Shao, L.Y., Mu, Y., Hu, Y., 2014, Oxidative capacities of size–segregated haze particles in a residential area of Beijing. *Journal of Environmental Sciences 26*, 167-174.

Tan, J.H., Duan, J.C., Zhen, N.J., He, K.B., Hao, J.M., 2016, Chemical characteristics and source of size-fractionated atmospheric particle in haze episode in Beijing. *Atmospheric Research 167*, 24-33.

Tang, Z.J., Hu, X., Qiao, J.Q., Lian, H.Z., 2018, Size distribution, bioaccessibility and health risks of indoor/outdoor airborne toxic elements collected from school office room. *Atmosphere 9*, 340-353.

Tao, J., Zhang, L.M., Zhang, R.J., Wu, Y.F., Zhang, Z.S., Zhang, X.L., Tang, Y.X., Cao, J.J., Zhang, Y.H., 2016, Uncertainty assessment of source attribution of $PM_{2.5}$ and its water-soluble organic carbon content using different biomass burning tracers in positive matrix factorization analysis-a case study in Beijing, China. *Science of the Total Environment 543*, 326-335.

Tian, L.W., Lucas, D., Fischer, S.L., Lee, S.C., Hammond, S.K., Koshland, C.P., 2008, Particle and gas emissions from a simulated coal-burning household fire pit. Environmental Science and Technology 42, 2503-2508.

Thurston, G.D., Burnett, R.T., Turner, M.C., Shi, Y., Krewski, D., Lall, R., Ito, K., Jerrett, M., Gapstur, S.M., Diver, W.R., Pope, C.A., 2016, Ischemic heart disease mortality and long-term exposure to source-related components of U.S. fine particle air pollution. *Environmental Health Perspectives*

124, 785-794.

Wang, J., Shao, L.Y., Wang, H., Spiro, B., Large, D.J., 2018, SHRIMP zircon U-Pb ages from coal beds across the PermianeTriassic boundary, eastern Yunnan, southwestern China. *Journal of Palaeogeography-ENGLISH* 7(2): 117-129.

Wang, Q.X., Tan, Z.Y., Zhao, H., Li, J. H., Tian, L. W., Wang, Q.Y., 2017, Species of iron in size-resolved particle emitted from Xuanwei coal combustion and their oxidative potential. *Environmental Science 38*, 2273-2279. (in Chinese with English abstract)

Wang, Y., Peng, L., Li, L.J., Wang, Y.X., Zhang, T., Liu, H.L., Mu, L., 2016, Chemical Compositions and Sources Apportionment of Re-suspended Dust in Jincheng. *Environmental science 37*, 82-87. (in Chinese with English abstract)

Wang, W.H., Shao, L.Y., L, J., Chang, L.L., Zhang, D.Z., Zhang, C.C., Jiang, J.K., 2019, Characteristics of individual particles emitted from an experimental burning chamber with coal from the lung cancer area of Xuanwei, China. *Aerosol and Air Quality Research 19*, 355–363.

Wang, T., Rovira, J., Sierra, J., Chen, S.J., Mai, B.X., Schuhmacher, M., Domingo, J.L., 2019, Characterization and risk assessment of total suspended particles (TSP) and fine particles ($PM_{2.5}$) in a rural transformational e-waste recycling region of Southern China. *Science of the Total Environment 692*, 432-440.

Xing, J.P., Shao L.Y., Zhang, W. B., Peng, J.F., Wang, W.H., Shuai, S.J., Hu, M., Zhang, D.Z.,2020, Morphology and size of the particles emitted from a gasoline-direct-injection-engine vehicle and their ageing in an environmental chamber. *Atmos. Chem. Phys. 20*, 2781–2794.

Xu, H. H., Wang, Y. S., Wen, T. X., He, X. X., 2007. Size distributions and vertical distributions of metal elements of atmospheric aerosol in Beijing. *Environmental Chemistry, 26(5)*, 675－679.

Xue, X., Chen, J., Sun, B., Zhou, B., Li, X., 2018, Temporal trends in respiratory mortality and short-term effects of air pollutants in Shenyang, China. *Environmental Science and Pollution Research 25,* 11468-11479.

Yang, K., Huang, Y., Zhao, G., Lei, Y., Wang, K., 2010, The expression of PAH–DNA adducts in lung tissues of Xuanwei female lung cancer patients. *Sino–German Journal of Clinical Oncology: English Edition 09*, 497 – 501.

Zelikoff, J.T., Schermerhorn, K.R., Fang, K., Cohen, M.D., Schlesinger, R.B., 2002, A role for associated transition metals in the immunotoxicity of inhaled ambient particulate matter. *Environmental Health Perspectives 110*, 871-875.

Zhang, R.C., Hao, X.J., Zhang, W.C., Liu, P.W., Ma, J., Shang, Y., Wu, M.H., Lv, S.L., 2016, Distribution of PAHs in size-resolved particles emitted from Xuanwei C1 coal combustion and their health risk assessment. *Asian Journal of Ecotoxicology 11*, 580-585.

Zhou, X.T., He, X.Z., 2006, The influence of indoor air pollution on chronic obstructive pulmonary disease (COPD). *China Environmental Science 26*, 591-594. (in Chinese with English abstract)

Figures

Tables

Table 1 Meteorological conditions during the sampling periods in Hutou and Xize villages in winter and spring.

Table 2 The PM mass concentration (μg/m^3) of size-segregated particles in Hutou and Xize villages in winter and spring.

Table 3 Plasmid DNA damage rate induced by size-segregated airborne particles at 250μg/mL for samples in Hutou and Xize villages in winter and spring.

Table 4 Correlation between water-soluble trace elements (μg/g) and DNA damage rate at 250μg/mL for the size-segregated particles in Hutou and Xize villages in winter and spring.

Table 5 The total water-soluble element mass concentration (ng/m^3) of size-segregated particles in Hutou and Xize villages in winter and spring.

Table 6 The comparison of the water-soluble trace elements in different area (Unit: ng/m^3)

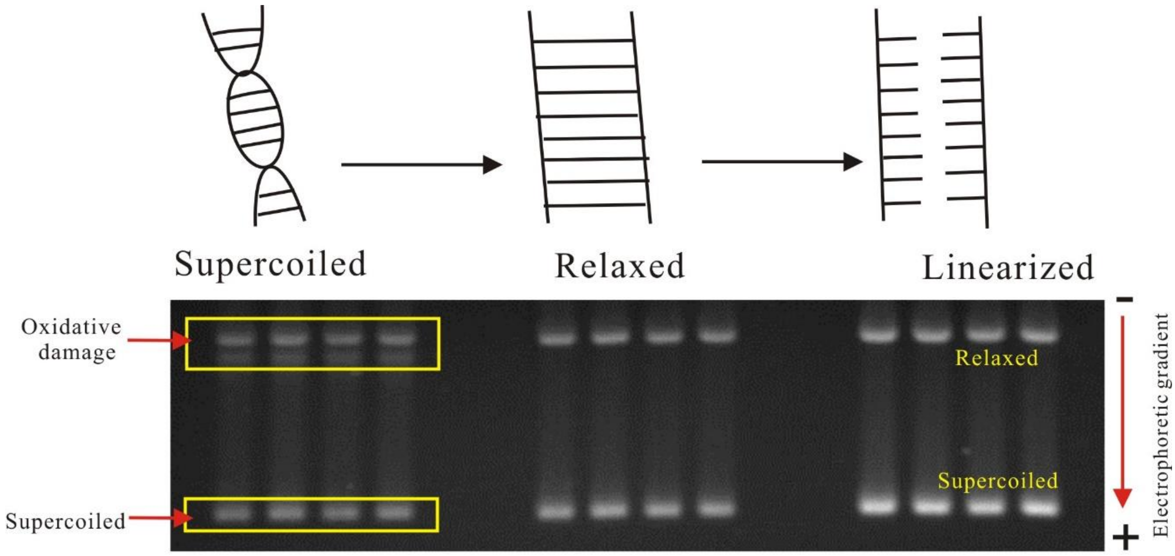

Fig. 1. DNA Plasmid Scission Assay

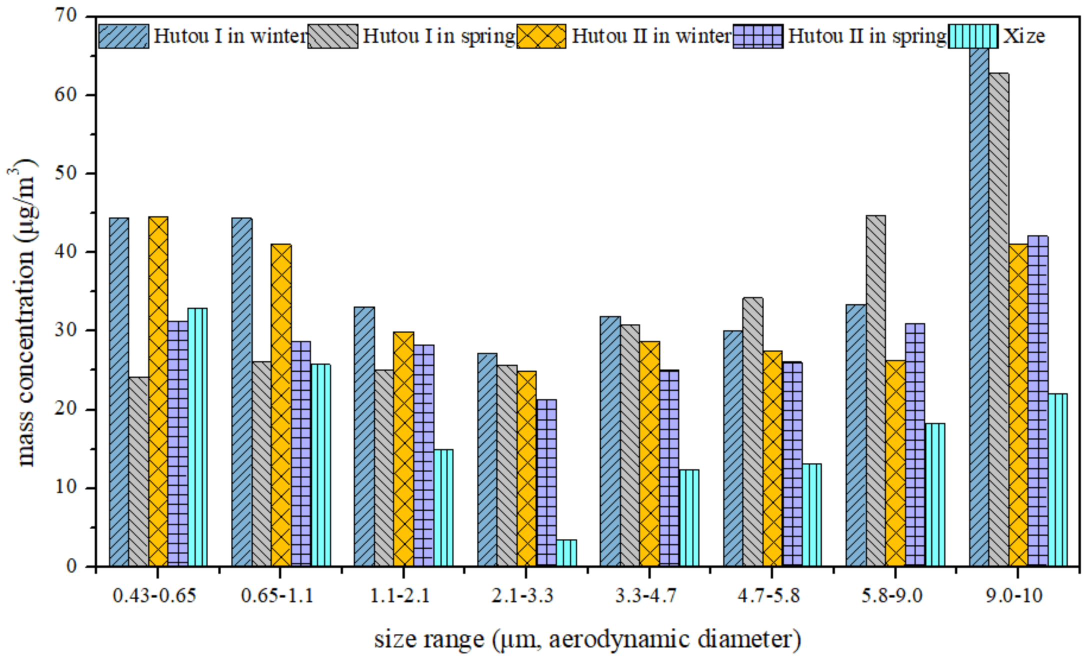

Fig. 2 Mass concentrations of particulate matter with different particle sizes in Hutou and Xize villages in winter and spring.

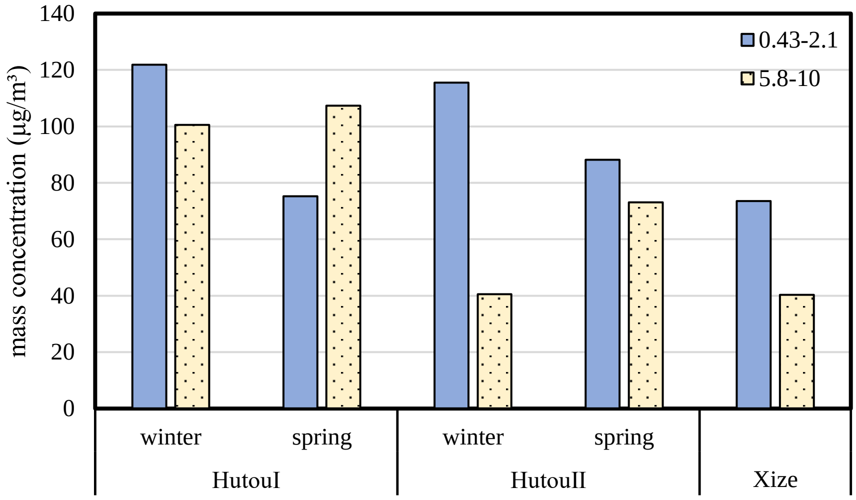

Fig. 3 Particle mass concentration with small and large size ranges in Hutou and Xize villages

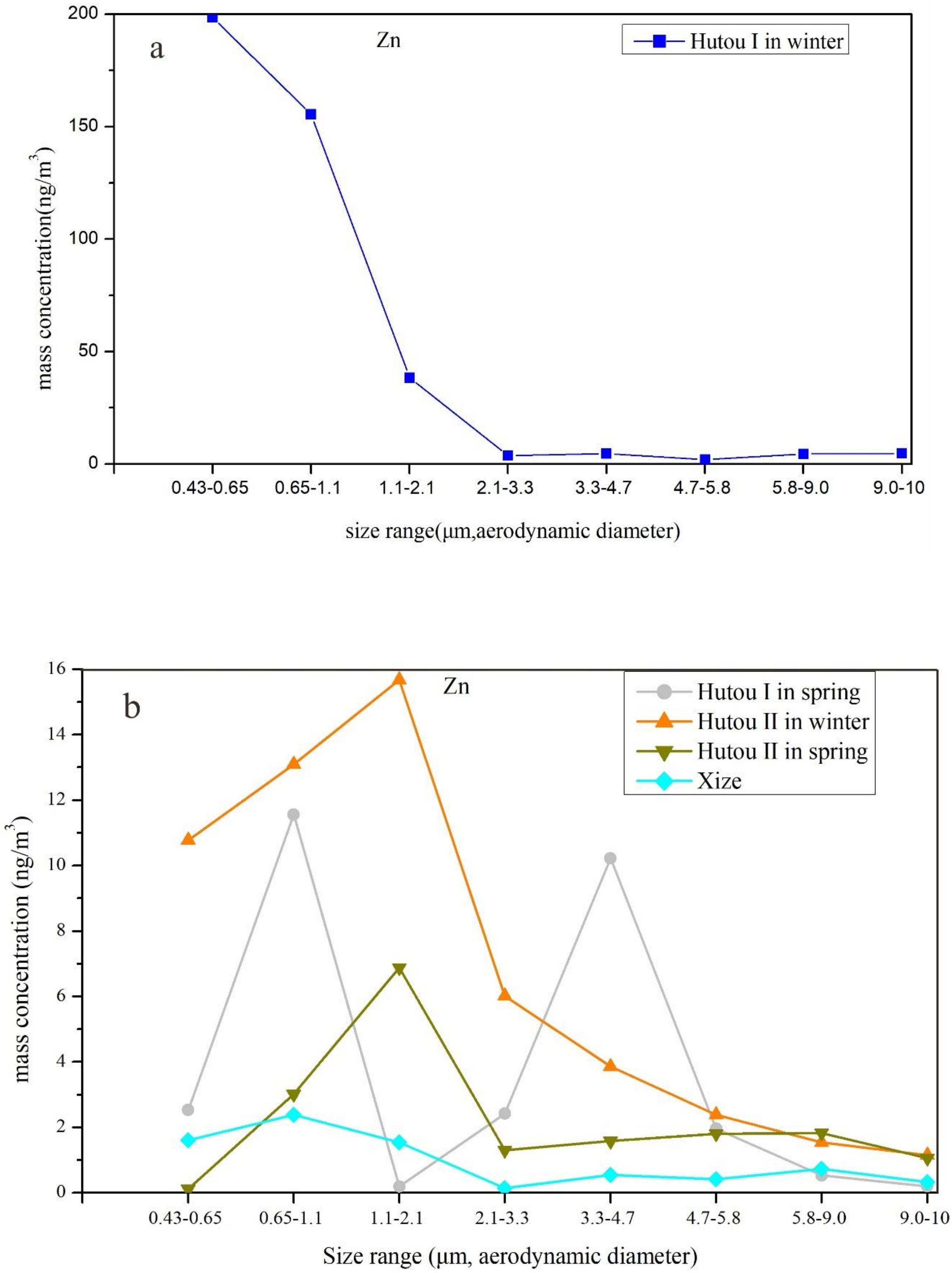

Fig. 4 Mass-size distributions of water-soluble trace element Zn with different particle sizes in Hutou and Xize villages in winter and spring

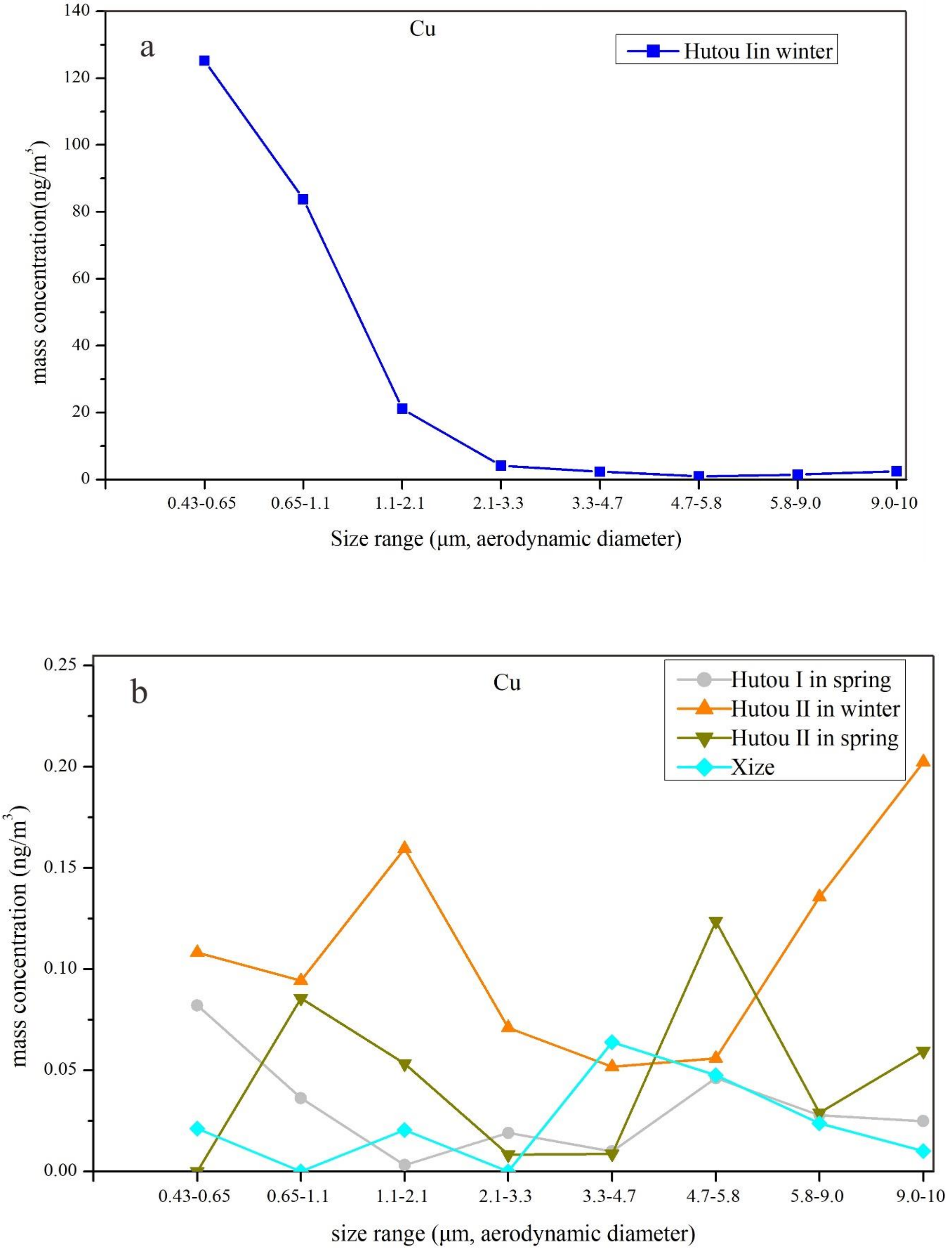

Fig. 5 Mass-size distributions of water-soluble trace element Cu with different particle sizes in Hutou and Xize villages in winter and spring

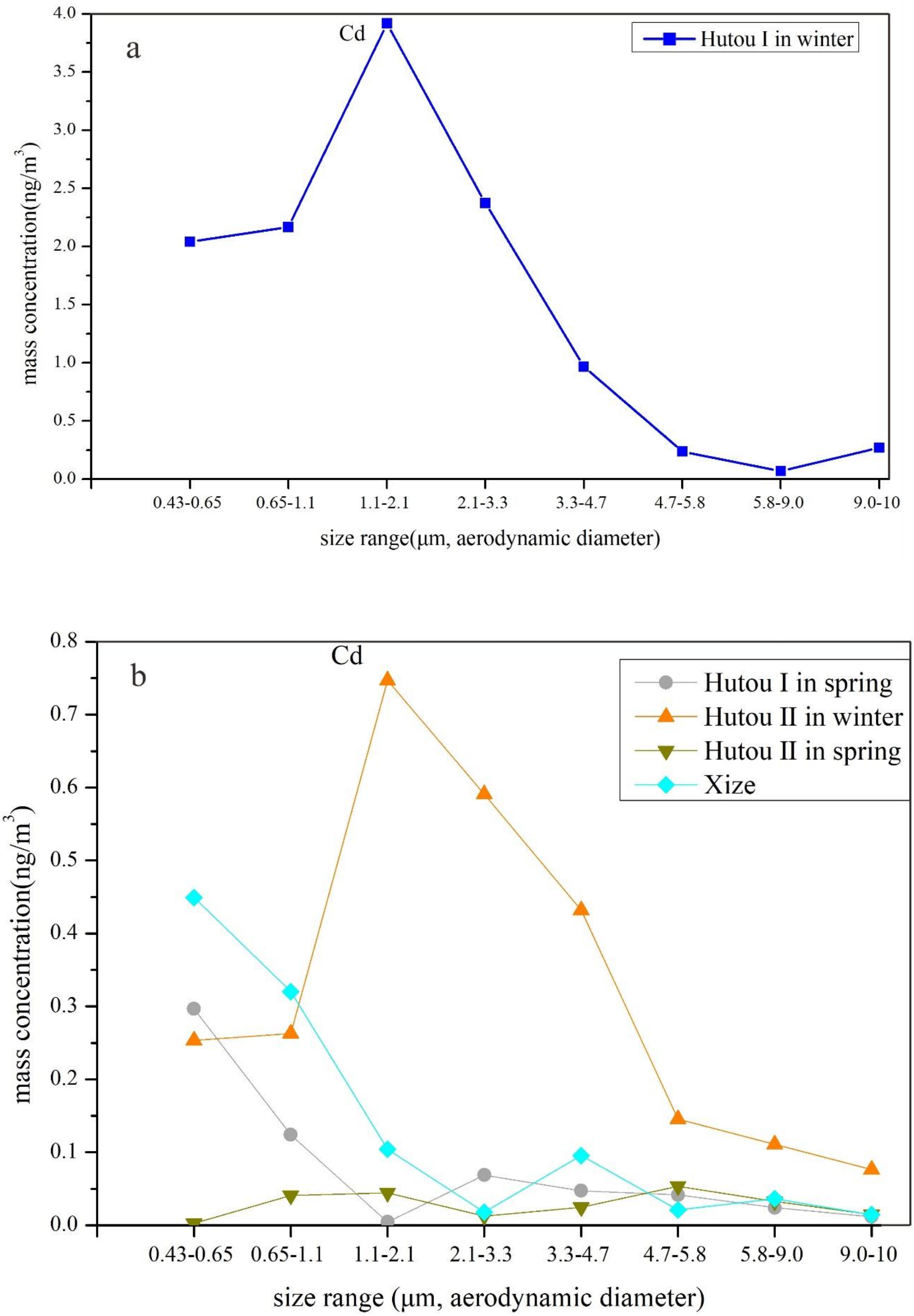

Fig. 6 Mass-size distributions of water-soluble trace element Cd with different particle sizes in Hutou and Xize villages in winter and spring

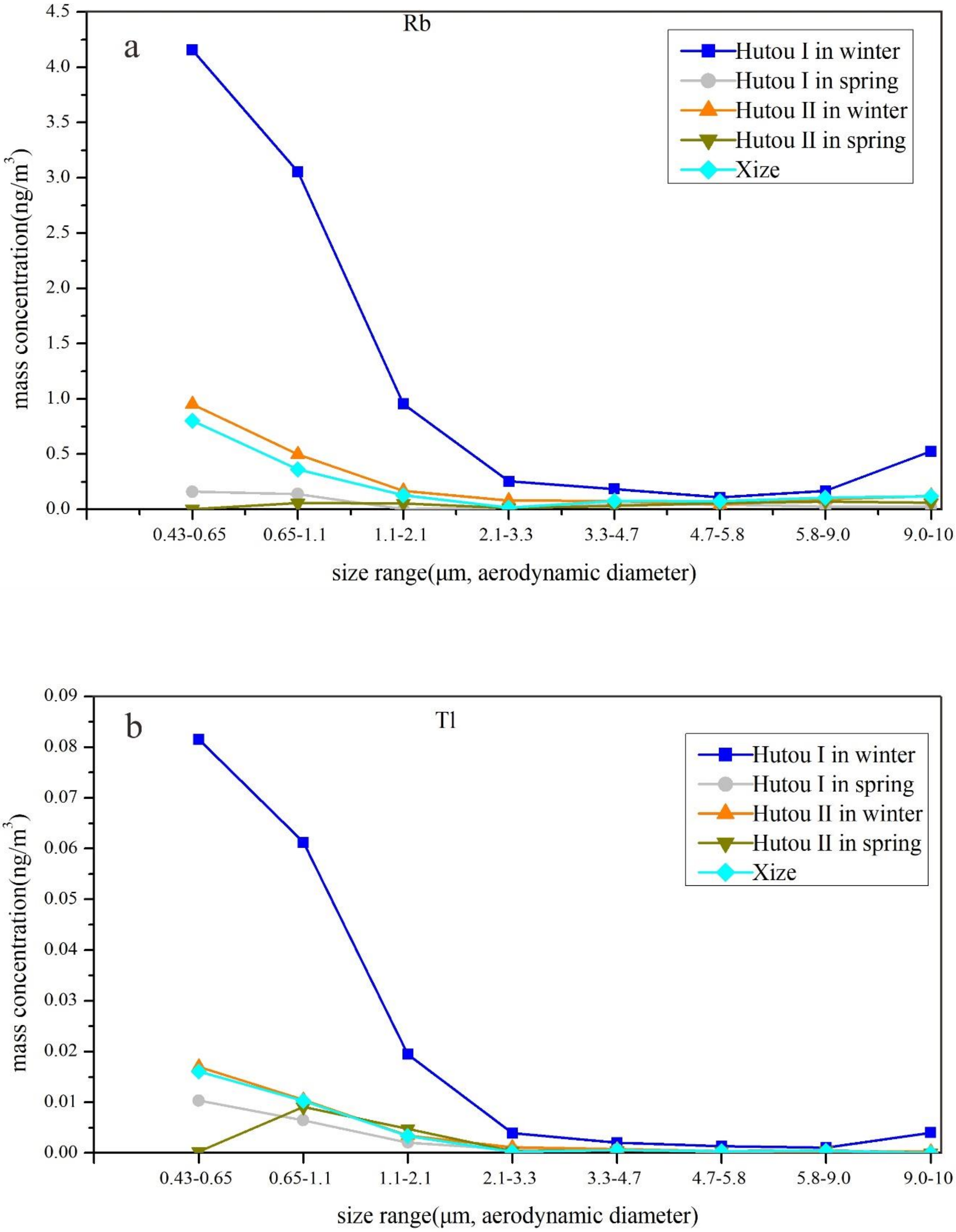

Fig. 7 Mass-size distributions of water-soluble trace elements Rb and Tl with different particle sizes in Hutou and Xize villages in winter and spring

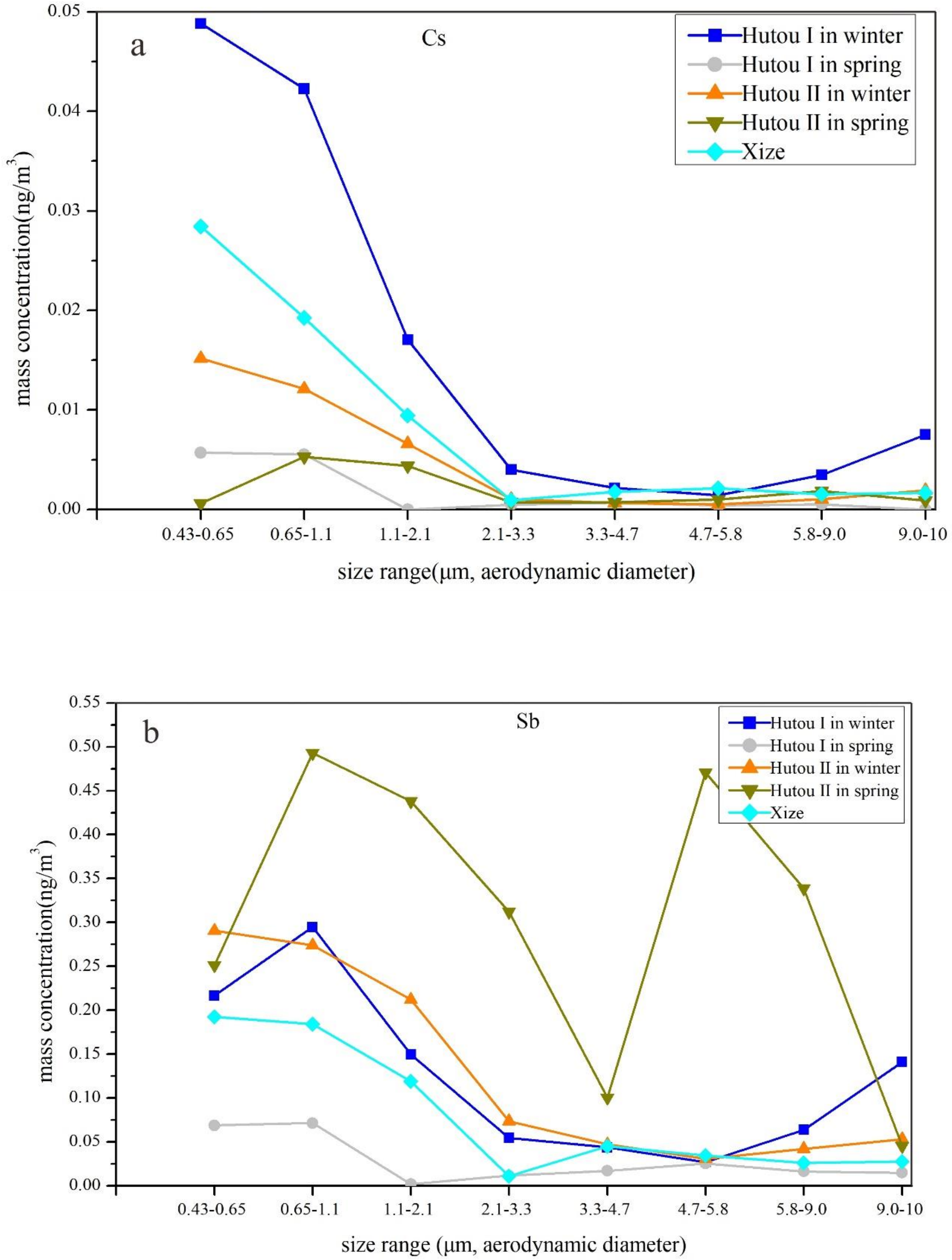

Fig. 8 Mass-size distributions of water-soluble trace elements Cs and Sb with different particle sizes in Hutou and Xize villages in winter and spring

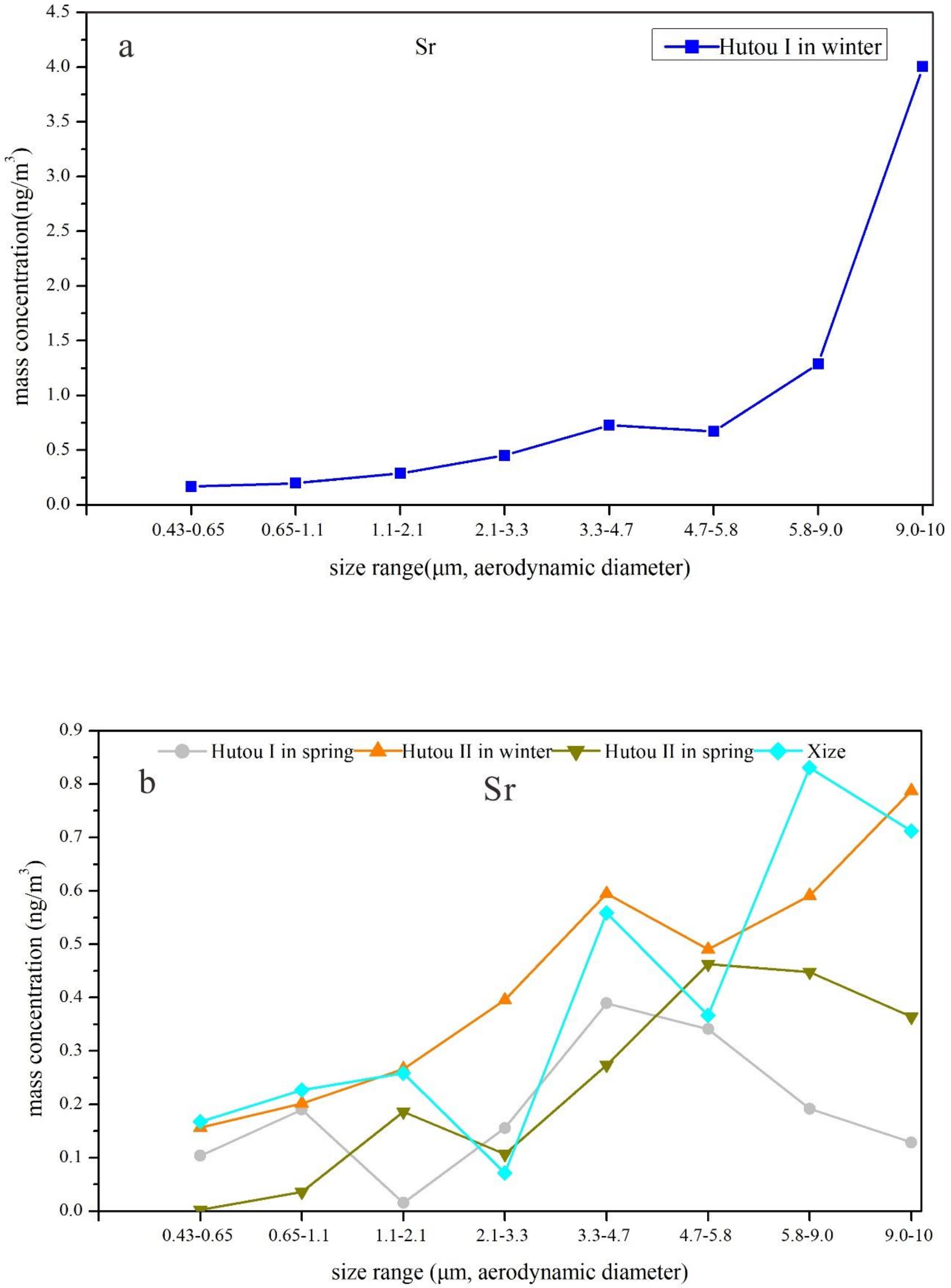

Fig. 9 Mass-size distributions of water-soluble trace element Sr with different particle sizes in Hutou and Xize villages in winter and spring

Table 1 Meteorological condition during the sampling periods in Hutou and Xize villages in winter and spring

Number	Sampling period	Sampling times	Average temperature(℃)	Relative humidity (%)	Average pressure(hPa)	Sample sites
1	2016.12.20-2016.12.22	9:00am-8:00am	14.9	59.4	805.3	Hutou I
2	2016.12.24-2016.12.26	9:00am-8:00am	12.1	65.2	801.8	Hutou II
3	2016.12.26.-2016.12.28	10:00am-8:00am	13.4	56.3	814.2	Xize
A	2019.3.1-2019.3.3	8:00am-8:00am-	14.6	54.5	818.5	Hutou I
B	2019.3.3-2019.3.5	8:00am-8:00am	14.0	45.3	816.5	Hutou II

Table 2 The PM mass concentration (μg/m³) of size-segregated particles in Hutou and Xize villages in winter and spring

Particulate sizes (μm)	Hutou I		Hutou II		Xize
	winter	spring	winter	spring	
0.43-0.65	44.39	24.17	44.56	31.31	32.93
0.65-1.1	44.39	26.12	41.05	28.69	25.74
1.1-2.1	33.09	24.98	29.87	28.23	14.88
2.1-3.3	27.1	25.63	24.86	21.29	3.51
3.3-4.7	31.92	30.82	28.7	24.99	12.37
4.7-5.8	30.09	34.23	27.53	26.07	13.04
5.8-9.0	33.42	44.61	26.2	31.01	18.22
9.0-10	67.17	62.78	41.05	42.11	22.06
total	311.57	273.32	263.83	233.7	142.75

Table 3 Plasmid DNA damage rate induced by size-segregated airborne particles at 250μg/mL for samples in Hutou and Xize villages in winter and spring

Particulate size (μm)	Hutou I (%)		Hutou II (%)		Xize (%)	blank
	winter	spring	winter	spring		
0.43-0.65	47.97	31.68	40.39	38.21	30.15	
0.65-1.1	49.43	35.72	42.47	33.04	33.23	
1.1-2.1	42.31	34.7	37.68	27.03	32.63	
2.1-3.3	38.12	31.34	36.28	28.91	32.01	
3.3-4.7	33.76	25.18	33.26	31.73	30.28	< 10
4.7-5.8	29.97	26.38	35.89	31.32	30.07	
5.8-9.0	33.67	27.43	33.07	37.42	22.06	
9.0-10	31.92	31.66	31.83	33.15	21.63	

Table 4 Correlation between water-soluble trace elements (μg/g) and DNA damage rate at 250μg/mL for the size-segregated particles in Hutou and Xize villages in winter and spring

The type of elements	total	Rb	Tl	Zn	Cu	Cs	Cd	Sb
Correlation coefficient	0.649^{**}	0.690^{**}	0.681^{**}	0.679^{**}	0.639^{**}	0.574^{**}	0.560^{**}	0.510^{**}
The type of elements	Pb	Sr	Sc	La	Ga	Y	Mn	Ti
Correlation coefficient	0.108	-0.418^{**}	-0.272	-0.262	-0.252	-0.240	-0.200	-0.198
The type of elements	V	Mo	Cr	Be	Nd	Li	Ba	Co
Correlation coefficient	-0.146	-0.161	-0.160	-0.118	-0.058	-0.044	-0.037	-0.031

** Significantly correlated at the 0.01 level (both sides).

Table 5 The total water-soluble element mass concentration (ng/m³) of size-segregated particles in Hutou and Xize villages in winter and spring

Particulate sizes (μm)	Hutou I		Hutou II		Xize
	winter	spring	winter	spring	
0.43-0.65	333.83	6.45	16.53	0.45	19.47
0.65-1.1	249.12	15.44	18.51	6.15	21.69
1.1-2.1	68.57	1.71	21.47	10.56	17.9
2.1-3.3	15.4	4.06	10.14	2.62	2.93
3.3-4.7	13.44	14.61	8.95	3.55	12.57
4.7-5.8	9.02	4.77	6.26	5.8	10.46
5.8-9.0	21.31	1.71	7.06	6.06	6.43
9.0-10	44.15	0.53	8.74	2.88	4.63
total	754.84	49.29	97.66	38.07	96.08

Table 6 The comparison of the water-soluble trace elements in different area (Unit: ng/m^3)

Water-soluble elements	Harbin Liu (2010)	Guangzhou-electronic-waste recycling region* Wang et al., (2019)	Guangzhou-Background site* Wang et al., (2019)	Beijing* Tao et al., (2016)	Beijing Chang (2019)	Hutou Hu et al., (2016)	Hutou this study
Zn	**318**	**----**	**----**	**270**	**140**	**98**	**412**
Cd	**1**	**7**	**3**	**3**	**1**	**9**	**12**
Mn	33	22	30	78	24	21	12
Cu	**7**	**162**	**32**	**34**	**10**	**85**	**241**
Ni	2	31	79	4	1	82	----
Tl	----	1	1	2	1	0	0
Co	1	0	0	----	0	2	0
Cr	2	35	39	11	8	21	21
Cs	----	0	1	1	0	0	0
Sb	----	10	3	10	4	1	1
Sr	----	7	8	16	4	9	8
Rb	**----**	**3**	**4**	**9**	**3**	**3**	**9**
Ti	7	34	48	130	5	187	7
V	2	7	4	4	2	19	6
Ga	----	----	---	5	0	1	0
Pb	**51**	**94**	**30**	**143**	**16**	**30**	**2**
total	424	413	282	577	219	568	731

*The levels of elements are taken from the whole sample.